

# Effect of Ozone and Relative Humidity on the Heterogeneous Uptake of Octamethylcyclotetrasiloxane and Decamethylcyclopentasiloxane on Model Mineral Dust Aerosol Components

Juan G. Navea,<sup>†,‡</sup> Shihe Xu,<sup>§</sup> Charles O. Stanier,<sup>‡</sup> Mark A. Young,<sup>\*,†</sup> and Vicki H. Grassian<sup>\*,†,‡</sup>

Department of Chemistry, The University of Iowa, Iowa City, Iowa 52242, Department of Chemical and Biochemical Engineering, The University of Iowa, Iowa City, Iowa 52242, and Health and Environmental Sciences, Dow Corning Corporation, Midland, Michigan 48686-0994

Received: March 11, 2009; Revised Manuscript Received: May 1, 2009

We have carried out kinetic and reaction yield studies to determine the effect of O<sub>3</sub> on the heterogeneous reaction of two cyclic volatile methylsiloxanes (cVMS), octamethylcyclotetrasiloxane (D<sub>4</sub>) and decamethylcyclopentasiloxane (D<sub>5</sub>), with model mineral dust aerosol in order to obtain a better understanding of the atmospheric fate of cVMS. The heterogeneous chemistry was studied in an environmental reaction chamber using FT-IR spectroscopy to monitor the reaction progress. The uptake kinetics and the reaction extent for D<sub>4</sub> and D<sub>5</sub> in the presence of O<sub>3</sub> were quantified for two components of mineral dust aerosol, hematite and kaolinite. Some experiments with a carbonaceous particulate, carbon black, were also performed for D<sub>5</sub>. The relative humidity (RH) inside the chamber was varied to investigate the influence of surface adsorbed water on the heterogeneous chemistry of the dust samples. With the dust samples, but not carbon black, the coadsorption of O<sub>3</sub> introduced a new reaction pathway, characterized by a linear, zero-order, decay of both gas phase cVMS and ozone. The new pathway does not saturate on the time scale of our experiments. Elevated RH was observed to decrease the total uptake of cVMS and ozone by the end of the experiment, but the characteristic linear decay was still present. The atmospheric loss of cVMS due to heterogeneous uptake is enhanced due to O<sub>3</sub>, even at higher RH values, but the overall loss rate is reduced at RH values typical of the troposphere.

## Introduction

Cyclic volatile methylsiloxanes (cVMS) such as octamethylcyclotetrasiloxane (D<sub>4</sub>) and decamethylcyclopentasiloxane (D<sub>5</sub>) are silicon fluids with low viscosity, low water solubility,<sup>1</sup> and relatively high vapor pressure.<sup>2</sup> These compounds are released into the environment from different anthropogenic sources, such as the synthesis of high molecular weight poly(dimethylsiloxane) polymers (PDMS) and from personal care products, where cVMS are used as carriers or emollients.<sup>3</sup> In the environment, these siloxanes primarily partition into the gas phase and the volatilization of cVMS from both the aqueous phase and from soils has been investigated.<sup>1,4</sup> Studies carried out for aqueous systems showed fast partitioning into the gas phase which increased as organic and inorganic compounds were added to the aqueous phase, decreasing the cVMS solubility.<sup>5,6</sup> Literature reports on the volatilization from soils showed that partitioning into the atmosphere is competitive with degradation of cVMS and the extent of volatilization increased with increasing relative humidity (RH).<sup>7,8</sup> Because of the physical properties of cVMS and the influence of RH, it has been suggested that more than 90% of the total cVMS released into the environment is present in the atmosphere.<sup>9</sup> Thus, examining potential loss processes for cVMS in the atmosphere is critical to understanding the overall environmental fate of these compounds.

The major homogeneous loss mechanism for D<sub>4</sub> and D<sub>5</sub> in the atmosphere is thought to be initiated by OH radical attack.<sup>10,11</sup> The resulting atmospheric lifetimes of D<sub>4</sub> and D<sub>5</sub> can be estimated as 16 and 10 days, respectively, based on a hydroxyl radical concentration of  $\approx 10^6$  molecules cm<sup>-3</sup>, typical of the troposphere at midlatitudes.<sup>12,13</sup> In contrast, experiments have shown no evidence for cVMS loss in the presence of O<sub>3</sub>, suggesting a high stability toward ozone.<sup>14</sup> Studies of the reactivity of D<sub>4</sub> toward O<sub>3</sub> with the addition of UV light at wavelengths >290 nm revealed a very slow pseudo-first-order decay with a half-life that varied from 30 min to 2 h.<sup>15</sup> The presence of water vapor in these experiments suggests that OH radicals generated from O<sub>3</sub> photolysis were responsible for the observed cVMS decay.

An alternative loss mechanism for atmospheric cVMS involves heterogeneous chemistry on the surface of reactive mineral dust aerosol. For example, degradation of siloxanes on various soils, particularly those with high clay content, has been previously observed.<sup>7,8,16</sup> Related chamber studies measured significant uptake of D<sub>5</sub> by Arizona road dust, which also has a large clay component.<sup>17</sup> Mineral dust represents a major fraction of the total aerosol loading in the troposphere and provides a large surface area for potential heterogeneous reactions.<sup>18–20</sup> Our recent work has suggested a possible role for mineral dust aerosol in the heterogeneous decay of atmospheric D<sub>4</sub> and D<sub>5</sub>.<sup>21</sup> These studies showed evidence for significant reactivity of various aerosols, such as hematite and kaolinite, a clay, toward cVMS. The resulting high surface coverages indicate that a surface polymerization mechanism may be active. In the ambient atmosphere, the aerosol surface will

\* Authors to whom correspondence should be addressed.

<sup>†</sup> Department of Chemistry, The University of Iowa.

<sup>‡</sup> Department of Chemical and Biochemical Engineering, The University of Iowa.

<sup>§</sup> Health and Environmental Sciences, Dow Corning Corporation.

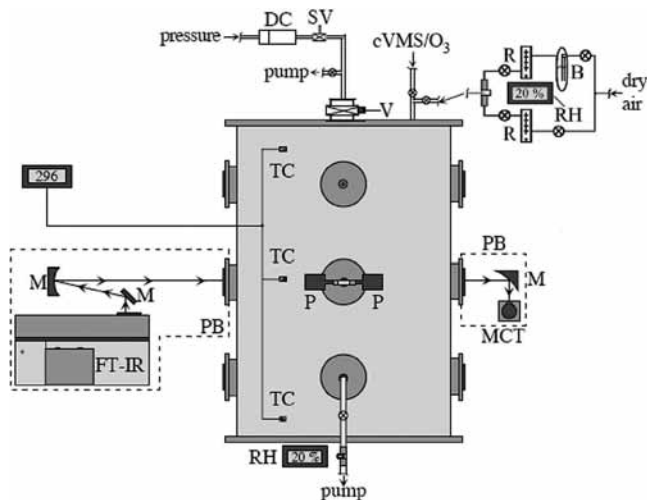


**Figure 1.** Schematic diagram of the environmental aerosol chamber and associated instrumentation showing the dust sample holder (DC), the solenoid valve (SV), the gate valve isolating the main chamber (V), the water bubbler (B), and flow meters (R) for the RH experiments, the IR spectrometer (FT-IR), and external beam path with mirrors (M) and detector (MCT) contained in purge boxes (PB). Relative humidity (RH), temperature (TC), and pressure (P) were monitored with appropriate transducers.

have coadsorbed species, most typically water. Our studies of RH dependence showed that cVMS uptake is reduced at higher RH and the kinetics of the initial uptake are slowed.

Other possible adsorbates of atmospheric relevance are oxidants, such as ozone, which may react directly with adsorbed cVMS or its products. Alternatively, ozone may indirectly effect the cVMS reaction by modifying the surface of the aerosol. Ozone is known to decompose catalytically on the surface of some mineral dusts, such as hematite,<sup>22</sup> possibly through intermediate surface oxide species.<sup>23–27</sup> There have been several reports of ozone reactions with organic<sup>26–30</sup> and inorganic species<sup>31</sup> adsorbed on surfaces. These reactions are thought to follow a Langmuir–Hinshelwood type mechanism whereby both reactants, or intermediate product species, are adsorbed on the surface. The confounding effects of oxidants, such as O<sub>3</sub>, on the heterogeneous chemistry of cVMS have not been previously explored.

As discussed, in a recent study, we have described a potential role for mineral dust aerosol in the heterogeneous loss of atmospheric cVMS.<sup>21</sup> Thus, in order to further explore the heterogeneous atmospheric fate of cVMS, we have investigated the synergistic effects of ozone and RH on the heterogeneous uptake of cVMS by representative mineral dust aerosol and carbon black. The reactions were carried out in an atmospheric reaction chamber using IR spectroscopy to probe the reaction extent and quantify the uptake kinetics. These results have significance for the current understanding of the environmental fate of cVMS and the major degradation pathways dictating their lifetime in the atmosphere.

## Experimental Section

The studies were carried out in an environmental aerosol reaction chamber using spectroscopic probes to follow the reaction progress. The chamber, which has been previously described,<sup>32</sup> is schematically diagrammed in Figure 1. It is a stainless steel cylinder with a total volume of 0.15 m<sup>3</sup> and a surface to volume ratio of 10.7 m<sup>-1</sup>, which has been internally coated with FEP Teflon. All of the chamber mating flanges are

Teflon coated, and connections to the chamber are fabricated from either Teflon or glass. The resultant chemically inert surfaces minimize the loss of gas phase reactants due to wall reactions. Spectroscopic access to the chamber is provided by appropriate windows mounted on side arms. The chamber is evacuated with a trapped mechanical pump. A glass manifold is used to introduce gas-phase reagent species, fill the chamber with buffer gas, and control the RH of the chamber contents.

A Fourier transform infrared (FT-IR) spectrometer (Mattson Infinity 60 AR) was employed to monitor the concentration of gas phase species inside the chamber. The IR beam is coupled into the chamber through Ge windows in a single-pass configuration using a series of gold-coated mirrors and then focused with an off-axis parabolic mirror onto an external MCT detector. The use of germanium windows reduces complications associated with the reactivity of inorganic salt windows, particularly at higher RH. The external IR beam path is continuously purged with dry air from a commercial gas generator (Whatman, 75-62). The output of the generator, humidified to the desired level, is also used to provide buffer gas for the chamber. The effective probe beam path length for the FT-IR spectrometer is 56 cm. Typically, IR spectra are collected at 8 cm<sup>-1</sup> resolution for 256 scans, resulting in a temporal resolution of 0.8 min.

In preparation for an experiment, the environmental aerosol chamber is evacuated to a base pressure of ≈20 mTorr. The evacuated chamber is backfilled with D<sub>4</sub> or D<sub>5</sub> vapor from the sample line to some nominal pressure which is confirmed using a Beer's law calibration. The initial pressures employed were typically at, or very near, the saturation vapor pressures of 550 mTorr (725 ppm) and 290 mTorr (380 ppm) for D<sub>4</sub> and D<sub>5</sub>, respectively. An ozone mixture is prepared by flowing oxygen (Air Products, USP grade) through an electric discharge ozone generator (OREC, model O3V5-O) and into the chamber until the desired O<sub>3</sub> concentration is obtained. The ozone concentration is quantified in the IR using a previously reported absorptivity.<sup>33</sup> The total chamber pressure is then brought up to ≈760 Torr with dry or humidified air. The humidity of the buffer is adjusted by passing the purge gas through a water bubbler and measuring the RH with a solid state sensor. However, the final RH is more precisely determined by a Beer's law calibration combined with measurement of the chamber temperature. The error in RH is estimated to be between 1 and 2% and dry conditions are specified as ≤1% RH, representing a lower limit to our detection sensitivity for the water absorbance features. The resultant gas mixture is allowed to equilibrate and mix in the chamber for approximately 1–2 h in order to quantify any possible wall losses and characterize reactions arising from homogeneous processes. Reference experiments were also conducted with single component mixtures (e.g., O<sub>3</sub> only) at various RH settings in order to further quantify wall losses, which were found to be negligible.

The powder dust samples (with different masses, depending on the surface area of the powder) are loaded into a small cartridge connected to the top flange of the environmental aerosol chamber and separated from the main chamber by a gate valve. In order to remove residual water from the powders, the cartridge is continuously evacuated by a trapped mechanical pump for approximately 3 h. The sample cartridge is connected to a high-pressure (≈100 psig) inert gas source through a fast acting solenoid valve. To initiate an experiment, the gate valve is opened and the solenoid valve is activated for a controlled time period (typically, 1 s), rapidly forcing the powder out of the cartridge and through a conical nozzle. A highly polished partial impactor plate positioned close to the nozzle exit results

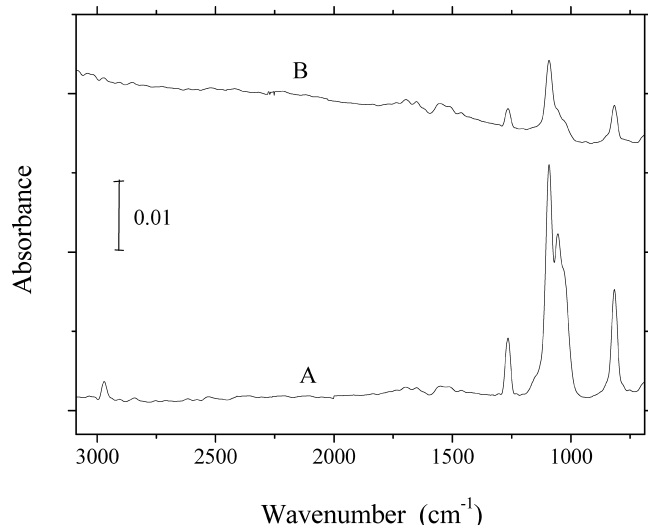


**Figure 2.** Representative FTIR spectra showing the chamber contents with  $D_4$  and  $O_3$  (85 ppm) under dry,  $\leq 1\%$  RH, conditions before aerosol introduction (A) and after 2 h of reaction time, (B). A decrease in both  $D_4$  and  $O_3$  bands is evident.

in efficient deagglomeration and dispersal of the powder into the chamber. The resulting turbulence rapidly mixes the chamber contents in less than 1 min.

The powder samples used in the current study were obtained from commercial sources: hematite ( $\alpha\text{-Fe}_2\text{O}_3$ , Aldrich, 99+ %), kaolinite (Alfa Aesar, 99+ %), and carbon black (Degussa FW-2, 99.98+ %). An X-ray analysis confirmed the mineralogy of the inorganic samples, and electron microscopy images were collected to qualitatively examine particle shape and size. An automated multipoint Brunauer–Emmet–Teller (BET) analysis (Quantochrome Nova 1200) was used to measure BET specific surface areas of  $2.8\text{ m}^2\text{ g}^{-1}$  for hematite,  $6.4\text{ m}^2\text{ g}^{-1}$  for kaolinite, and  $460\text{ m}^2\text{ g}^{-1}$  for carbon black. The BET area, determined using  $N_2$ , represents an upper limit to the reactive surface area available on each powder. The mass of each dust sample was adjusted so that the total BET specific surface area introduced into the chamber is approximately the same in each experiment,  $\approx 8.0\text{ m}^2$ . In addition, a primary particle size of 13 nm was specified for carbon black,<sup>35</sup> while measurements with a commercial particle sizer (APS) of hematite and kaolinite particles show a peak in the distribution near 300 nm, 140 nm, respectively.<sup>34</sup> The cVMS samples, provided by our Dow Corning collaborators, were tested for purity by sampling both the liquid and the head space with GC-MS (ThermoElectron) using a Restek Rxi-1 ms column (15m length and 0.32 mm i.d.) with a nonpolar phase (Crossbond 100% dimethylpolysiloxane). Both siloxane samples were found to be  $>99.5\%$  pure.

## Results

Figure 2 shows typical IR spectral data for an experiment with  $D_4$ ,  $O_3$ , and hematite as the dust sample, collected under dry,  $\leq 1\%$  RH, conditions. The spectrum recorded before introduction of the aerosol, Figure 2A, exhibits a band at  $1054\text{ cm}^{-1}$  ascribed to  $O_3$  along with four absorbance features due to  $D_4$ : a C–H methyl stretching mode at  $2900\text{ cm}^{-1}$ , a scissoring mode at  $1275\text{ cm}^{-1}$ , a Si–O stretching mode at  $1090\text{ cm}^{-1}$ , and a methyl rocking mode at  $890\text{ cm}^{-1}$ . The  $D_5$  spectrum is very similar in appearance. The peak absorbance at  $1054\text{ cm}^{-1}$  was used to quantify the ozone concentration,<sup>36,37</sup> and the methyl scissor feature at  $1275\text{ cm}^{-1}$  was integrated to determine the concentration of cVMS by referencing a Beer's law calibration

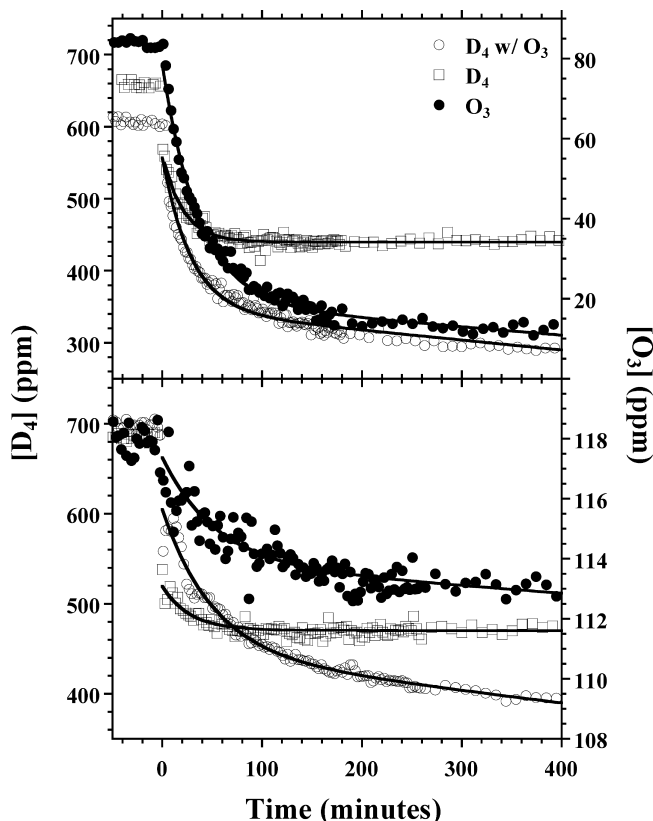


**Figure 3.** Time resolved data for  $D_4$  and  $O_3$  in mixture experiments when exposed to hematite, top panel, and kaolinite, bottom panel, dust samples under dry, 1% RH, conditions. Included, are data from a reference experiment with only  $D_4$  in the chamber. The solid lines represent fits to the experimental data. Dust loadings have been adjusted so that the same BET surface area is available in each experiment, as described in the text.

(vide supra). Continuous spectral monitoring of the chamber contents during the prereaction period showed no indication of reaction between the cVMS and  $O_3$  in the absence of aerosol, and wall losses were found to be negligible. The spectrum in Figure 2B was recorded after introduction of the dust sample and corresponds to a reaction time of several hours. The sloping baseline is due to nonresonant scattering of the probe beam by the suspended particulates. There is clear evidence for an intensity reduction in the  $D_4$  and  $O_3$  absorption bands, signifying a reactive loss pathway facilitated by the presence of the mineral dust. No new IR absorption features were observed to grow in over the spectral range  $5000\text{--}650\text{ cm}^{-1}$ , indicating either that gas-phase reaction products are not formed or that any possible products are IR inactive or weak absorbers.

Spectral data collected before and after the introduction of the powder sample into the chamber were analyzed to determine the time dependence of gas-phase reactant concentrations. The results for  $D_4$  and  $O_3$  reactions with hematite and kaolinite dust samples are presented in Figure 3. For comparison, we have also included data from reference experiments with mineral dust and  $D_4$  but without added ozone. The results of these latter experiments are in accord with our previous report of cVMS interactions with mineral dust.<sup>21</sup> The reactivity of a dust toward cVMS can be characterized in terms of the reaction extent, measured as the fraction of the initial siloxane that has reacted by the end of the experiment (400 min), and the apparent uptake coefficient,  $\gamma_{\text{app}}$ . The uptake coefficient, the fraction of gas–surface collisions that lead to loss of cVMS, quantifies the kinetics of the heterogeneous uptake process. The uptake



coefficient is calculated according to

$$\gamma_{\text{app}} = \frac{4}{\bar{c}S_{\text{BET}}\tau[C_{\text{mass}}]} \quad (1)$$

where  $\bar{c}$  is the mean speed of cVMS ( $\text{m s}^{-1}$ ),  $C_{\text{mass}}$  is the mass concentration of dust in the chamber ( $\text{g m}^{-3}$ ), and  $S_{\text{BET}}$  is the specific surface area of the dust ( $\text{m}^2 \text{g}^{-1}$ ), previously measured by a BET analysis. The characteristic cVMS decay time,  $\tau = 1/k$ , is determined from a fit of the experimental data, as indicated by the solid lines in Figure 3. Note that in this figure and all subsequent figures showing decay data, the powder mass in each experiment has been adjusted to yield the same surface area in the chamber (vide supra). Thus, the decay curves can be directly compared with each other.

In the absence of ozone, both mineral dusts exhibit significant reactivity as evidenced by the amount of  $D_4$  lost by the end of the experiment, about 40%. With addition of  $O_3$  the overall reaction extent is enhanced such that 55–65% of the  $D_4$  is consumed. More significantly, the kinetics of the uptake process are radically altered by ozone. The  $D_4$  concentration initially decays exponentially whether ozone is present or not. With  $O_3$  in the chamber, this initial decay is slightly slower (smaller  $\gamma_{\text{app}}$ ). However, instead of the surface saturation observed in the  $D_4$ -only experiments, there is evidence for continued heterogeneous reactivity as the gas phase  $D_4$  loss transitions to a linear decay at longer reaction times. The linear portion of the time course data is symptomatic of zero-order kinetics with continued consumption of  $D_4$  and, on the time scale of our experiments, no saturation of the dust surface. We have fit the  $D_4$  data from the ozone experiments to an exponential plus linear decay function, as shown by the solid lines in the figure.

The  $O_3$  decay curves are analogous to those of the siloxane, exhibiting an initial exponential decay followed by a linear loss that does not saturate. A similar decay function was used to fit the ozone data. While for both kaolinite and hematite the characteristic  $O_3$  decay times are very close to those of  $D_4$ , the slopes of the linear portions of the decay curves are quite different. Additionally, the overall uptake of  $D_4$  by either dust sample exceeds the amount of  $O_3$  lost from the gas phase. In the case of hematite, the ratio of overall  $D_4$  to  $O_3$  loss is about 4 after 400 min of reaction time. It is also clear that much less of the available ozone reacts on the kaolinite sample compared to the hematite (4% vs 86%).

A similar set of experiments was completed for  $D_5$ , with additional studies on carbon black aerosol, and the results are summarized in Figure 4. We have previously demonstrated that hematite and kaolinite are extremely reactive toward  $D_5$ , resulting in rapid and quantitative uptake of the gas-phase siloxane.<sup>21</sup> These findings are affirmed by the data for the cVMS-only experiments shown in Figure 4. The kaolinite sample is so reactive that all of the initial  $D_5$  is rapidly lost regardless as to whether ozone is present and it is not possible to detect whether there is any enhancement in the uptake. The hematite sample actually shows a 15% reduction in  $D_5$  uptake with  $O_3$  in the chamber. However, the  $D_5$  decay does transition to a linear decay regime, as was the case for  $D_4$  reacting with mineral dust in the presence of  $O_3$ . The continued reactivity of the hematite surface suggests that eventually all of the  $D_5$  would have reacted, yielding the same reaction extent as for the  $D_5$ -only experiment, albeit on a longer time scale.

The ozone decay kinetics and the consequent uptake on mineral dust are similar to the observations from the  $D_4$  experiments. For both dust samples, there is an initial expo-

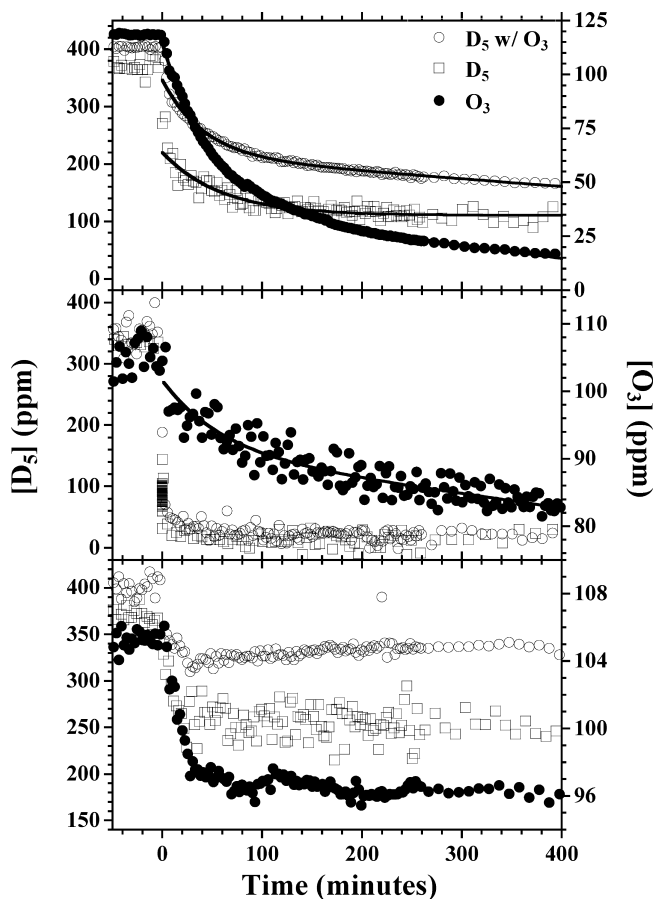


**Figure 4.** Time-resolved data for  $D_5$  and  $O_3$  in mixture experiments when exposed to hematite, top panel, kaolinite, middle panel, and carbon black, bottom panel, dust samples under dry, 1% RH, conditions. Included are data from reference experiments with only  $D_5$  in the chamber. The solid lines represent fits to the experimental data.

ponential decay of ozone that gives way to a linear decrease at longer times. The amount of  $D_5$  uptake is still larger than the  $O_3$  lost for both of the mineral dust surfaces studied although by a reduced margin. The ratio of overall  $D_5$  to  $O_3$  loss on hematite is about 2.1. Also, the extent of ozone loss is again, as for the  $D_4$  mixtures, larger on hematite than it is on kaolinite surfaces, 85% compared to 20%. Finally, the characteristic decay times for  $O_3$  and  $D_5$  on hematite are approximately equal. We have fit the mineral dust data to the appropriate loss functions, as illustrated in the figure.

The carbon black aerosol manifests quite different reactivity compared to the mineral dust samples studied. The surface rapidly saturates with respect to  $D_5$  uptake whether ozone is present in the chamber or not. The extent of  $D_5$  uptake with ozone is slightly reduced but the reaction still quickly saturates. Ozone itself also exhibits relatively small gas phase loss and rapid saturation of the surface. No longer time continued reactivity of the surface is evident for either the siloxane or the ozone.

The importance of relative humidity, a critical characteristic of the ambient atmosphere that can have a large effect on heterogeneous processes, was investigated for the hematite mineral dust sample. The RH of the buffer gas was varied from dry,  $\leq 1\%$  RH, conditions up to a maximum of about 60% RH in several steps. Time course data were recorded for both the cVMS and  $O_3$  gas phase species under these conditions. Results for the  $D_4/O_3$  system are summarized in Figure 5, and results for the  $D_5/O_3$  system are in Figure 6. For either cVMS and

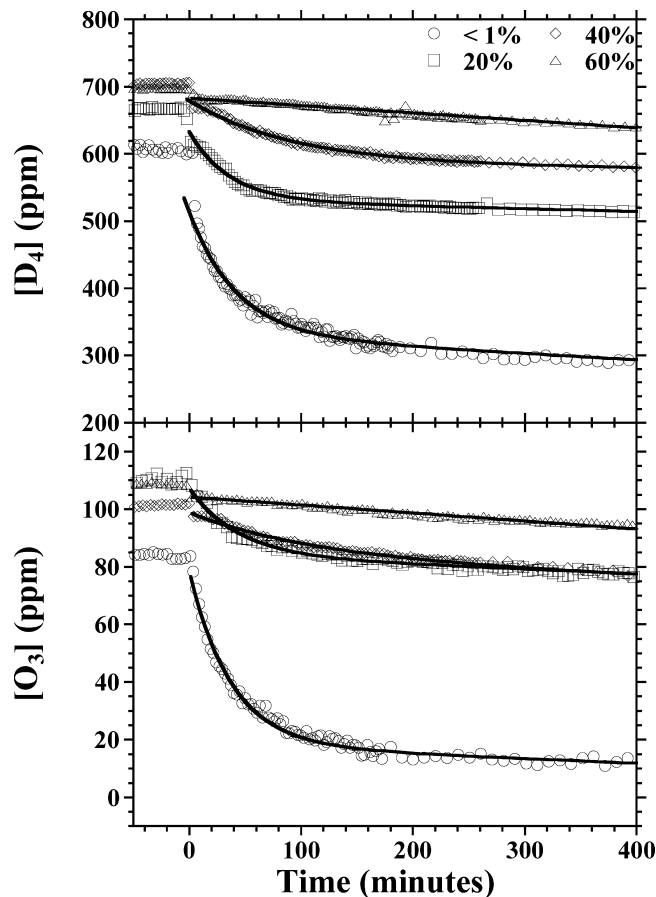


**Figure 5.** Time-resolved data for  $D_4$ , top panel, and  $O_3$ , bottom panel, in mixture experiments when exposed to hematite under various RH conditions. The solid lines represent fits to the experimental data.

any RH studied, there was no siloxane or ozone decay observed before the aerosol was introduced into the chamber (negative reaction times) and, thus, wall loss and homogeneous gas-phase chemistry were negligible.

The effect of RH on the reaction of  $D_4$  and  $O_3$  with hematite mineral dust is quite dramatic. Even relatively modest RH levels of 20% greatly reduce the uptake of both cVMS and  $O_3$  and increasing inhibition is observed up to 60% RH, the highest level studied. The initial exponential decay is evident at the lower RH values, but the characteristic decay times increase with increasing RH. The  $D_4$  and  $O_3$  characteristic decay times remain approximately equal for a given relative humidity. The contribution of the exponential decay component to the overall loss is markedly smaller with an increase in the RH. At 60% RH, the exponential decay is not even evident and we have simply fit the data for both reactants to a straight line under these conditions.

The data presented in Figure 6 for the  $D_5$  system present a qualitatively similar response to RH, showing a reduced uptake of both siloxane and ozone as the RH is increased. The  $D_5$  does not appear to be as sensitive to RH; at 20% RH the fraction of  $D_5$  reacted is only slightly reduced and it is not until RH values  $\geq 40\%$  that significant reduction in uptake is observed. The  $D_5$  is still more reactive than the  $D_4$  despite the RH effect and the fraction of  $D_5$  reacted is always larger than that of  $D_4$  under equivalent RH conditions. The RH effect on  $O_3$  in the  $D_5$  experiments parallels observations of the  $D_4$  system and the uptake is greatly lowered even at 20% RH and proportionally smaller reductions are measured at higher RH. The initial exponential decay time increases, and the exponential decay

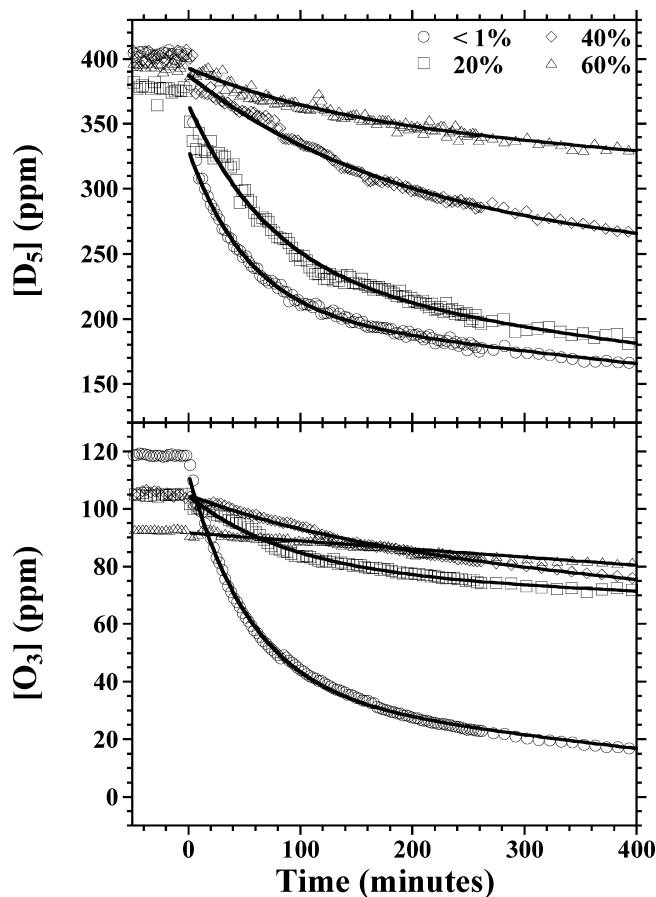


**Figure 6.** Time-resolved data for  $D_5$ , top panel, and  $O_3$ , bottom panel, in mixture experiments when exposed to hematite under various RH conditions. The solid lines represent fits to the experimental data.

component is smaller, for both  $D_5$  and  $O_3$  as the RH increases until the decay is largely zero order at 60% RH. The  $O_3$  data at 60% RH was fit to a straight line as the exponential component cannot be discerned.

## Discussion

In the absence of ozone and under dry conditions,  $\leq 1\%$  RH, we observe significant uptake of gas phase cVMS on the mineral dusts hematite and kaolinite. The  $D_5$  sample has a particular affinity for dust as there is 100% loss of the saturation vapor pressure. The carbon black sample is less reactive and the surface appears to be rapidly saturated, albeit after about 40% of the initial  $D_5$  has reacted. These results are consistent with our previous study of cVMS interactions with various mineral dust aerosol components.<sup>21</sup> The siloxanes are very reactive toward dust, in particular kaolinite, a clay, and hematite. The multilayer coverages that result suggest a polymerization mechanism for the adsorbed siloxane facilitated by active surface sites on the mineral dust.<sup>38</sup> The absence of gas-phase products in the IR data indicates that heterogeneous reaction yields nonvolatile products, such as polymers. We have also separately investigated  $O_3$  reactions with hematite and observed total loss of ozone through a surface-catalyzed process.<sup>22</sup> Heterogeneous decomposition of ozone produces molecular oxygen, undetectable via IR absorption, while possibly oxidizing the surface.<sup>23–27</sup>

The experiments with  $O_3$ -cVMS mixtures show no evidence for gas-phase reaction loss or losses mediated by the chamber walls. The lack of homogeneous reactivity is not surprising given that the siloxanes are saturated compounds and is consistent

**TABLE 1: Areal Rates for the Linear Component of the cVMS and O<sub>3</sub> Loss Curves under Dry Conditions, ≤ 1% RH, for Hematite and Kaolinite Samples<sup>a</sup>**

		areal rate (×10 <sup>10</sup> cm <sup>-2</sup> s <sup>-1</sup> )		
		cVMS	O <sub>3</sub>	R
hematite	D <sub>4</sub>	10 ± 2	1.2 ± 0.4	8 ± 5
	D <sub>5</sub>	2.4 ± 0.5	3.0 ± 0.7	0.8 ± 0.3
kaolinite	D <sub>4</sub>	11 ± 2	0.17 ± 0.04	63 ± 26
	D <sub>5</sub>	na	1.4 ± 0.4	na

<sup>a</sup> The ratio, *R*, of the cVMS to O<sub>3</sub> loss rates is also calculated for each experiment.

with previous studies.<sup>14</sup> When dust is introduced into the chamber, both O<sub>3</sub> and the cVMS are observed to decay, but the details of the loss process are modified from experiments where each gas reacts separately with dust, as seen in Figures 3 and 4. In the case of D<sub>4</sub>, the fraction reacted by the end of the experiment increases with ozone in the chamber. The D<sub>5</sub> experiments do not exhibit a similar enhancement, but the effect of O<sub>3</sub> is partially masked by the much higher reactivity of the D<sub>5</sub> toward mineral dust. D<sub>5</sub> reacts completely with a kaolinite surface whether O<sub>3</sub> is present or not, and the reaction extent is actually slightly decreased with ozone in the hematite experiments. The D<sub>5</sub> reaction with carbon black is also slightly suppressed.

In addition to effects on the reaction extent, the most significant change due to ozone is manifest in the details of the reaction kinetics. For each of the mineral dusts studied, and for either cVMS, the typical exponential decay due to siloxane uptake transitions to a linear loss regime at longer times. The ozone is also observed to decay linearly at longer reaction times in the mixture experiments. The longer time, linear decay is suggestive of zero-order kinetics as surface sites become saturated and reaction on the dust surface becomes rate limiting.

We can represent the uptake and reaction process as a two-step mechanism,



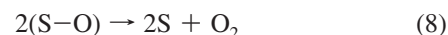
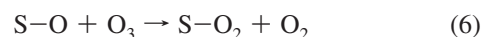
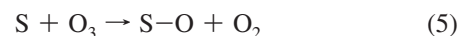
where *R* and *P* represent reactant and product species and *R*·*S* is a surface adsorbate intermediate. As the surface saturates, the adsorbed intermediate reaches a steady state, and the reaction becomes rate limited by eq 3 in a zero-order process. The observed reaction rate, *ν*, can be expressed in terms of a surface reaction rate constant, *k*<sub>sur</sub>, as

$$\nu = k_{sur} S n_s \quad (4)$$

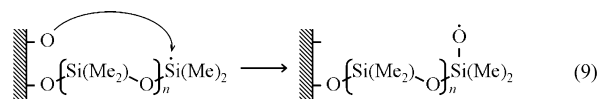
where *S* is the BET dust surface area concentration in the chamber and *n*<sub>s</sub> is the surface site density. Dividing the measured rate by *S* yields an areal rate constant, which we have listed in Table 1 for O<sub>3</sub> and the cVMS. The rates were determined from the slope parameter using an exponential plus linear fitting function or a direct, linear fit of the data, as described above. The fitting errors are propagated into the reported areal rates.

The linear decay shows that the mineral dust surface continues to be reactive toward cVMS and the reaction does not saturate as long as ozone is present. The implication, then, is that eventually all of the initial cVMS will react if there is sufficient ozone. Thus, the D<sub>4</sub> reaction extent should be enhanced with O<sub>3</sub> and eventually reach 100% for D<sub>5</sub>, even in the case of hematite dust which shows a reduced reactivity when defined in terms of our experimental reaction times. In our previous work, we speculated that a surface polymerization reaction led to irreversible loss of gas-phase cVMS and that the reaction would eventually terminate due to blocking of the active surface sites by product siloxanes.<sup>21</sup> Thus, we generally observed a single exponential decay of the gas-phase cVMS, consistent with eq 2, and we could extract *γ*<sub>app</sub>. In the mixture experiments, in contrast, we observe zero-order kinetics as eq 3 becomes rate limiting due to the saturation of reactive sites on the surface.

The observation of zero-order kinetics and the continued reactivity of the dust surface means that active surface sites must be regenerated in a catalytic process, as suggested by eq 3. Since we do not observe such behavior in the absence of ozone, it must be the O<sub>3</sub> that regenerates active surface sites, allowing the reaction to continue. These may be the same type of surface sites normally active in the absence of ozone or they may be new sites generated by the heterogeneous ozone reaction that are active toward siloxane degradation. Given the high siloxane surface coverages measured and the continued reactivity of the available surface area, it is more probable that the ozone is regenerating active surface sites in a catalytic process. The fact that O<sub>3</sub> also decays, at longer times, via a linear, zero-order process indicates that the relevant surface process involves adsorbed ozone or an ozone decomposition product on the surface. Ozone itself decays catalytically on hematite<sup>22</sup> and is thought to produce surface oxide and peroxide intermediates<sup>23–27</sup>



where *S* represents an active site and *S*–*O* and *S*–*O*<sub>2</sub> represent the product surface oxide and peroxide, respectively. Reaction 7 is thought to be relatively slow.<sup>26</sup> The reaction, then, would be of the Langmuir–Hinshelwood type, with both reactants adsorbed, rather than an Eley–Rideal mechanism, with one reactant adsorbed and the other reacting from the gas phase. It may be that the surface oxide produced from ozone decomposition reacts with a linear siloxane product bound on the surface to regenerate the active surface site and yield a siloxane fragment that can continue to polymerize.



Similar mechanisms have been proposed for heterogeneous decomposition of various organic and inorganic species in the presence of ozone.<sup>26,31</sup>

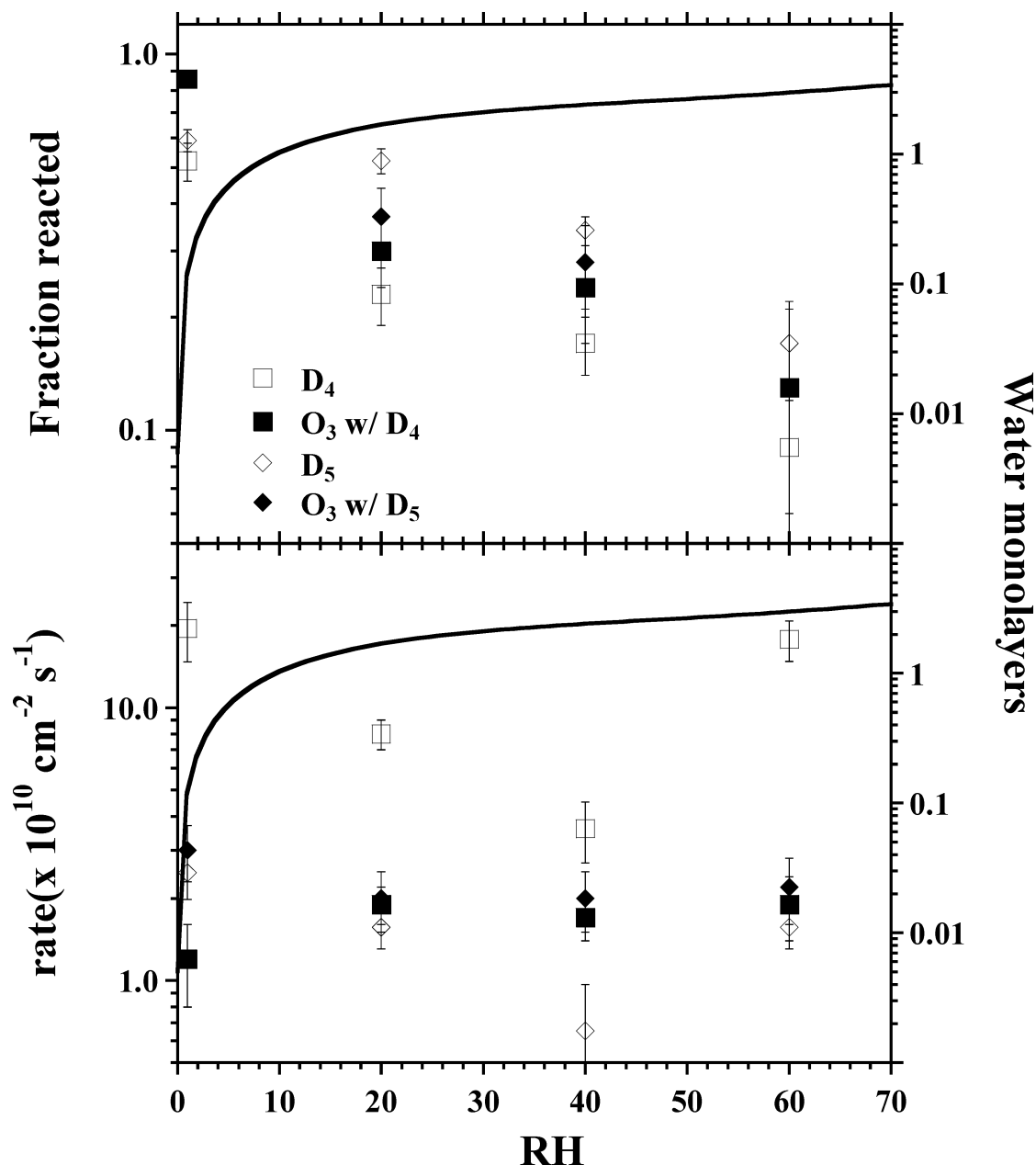


**Figure 7.** The top panel shows the fraction of the initial cVMS or O<sub>3</sub> that has reacted with hematite at the end of the experiment as a function of RH. The bottom panel shows the areal rates for both cVMS and O<sub>3</sub> with hematite as a function of RH. The solid line represents a fit to water uptake measurements on hematite reported in ref 22.

We have noted that the exponential decay component of the loss curves in Figures 4 and 5, reflective of the time it takes for the surface to saturate with respect to both species, are the same for both the cVMS and O<sub>3</sub> for a given dust. This suggests that adsorption of one species is rate limiting the uptake of the other species. If the ozone is regenerating sites active toward cVMS, then it is siloxane uptake that limits the initial O<sub>3</sub> decay. The amount of cVMS lost in the first few minutes of the reaction corresponds to 1–2 monolayers of surface coverage. The O<sub>3</sub> would adsorb and decompose on remaining open sites and subsequently regenerate new sites active toward siloxane uptake as well as more ozone. Some insight can be gained from examining the ratio of the cVMS to O<sub>3</sub> linear loss rates,  $R$ , as tabulated in Table 1. The D<sub>4</sub> results suggest that ozone is much more efficient at facilitating the siloxane reaction on kaolinite surfaces,  $R = 63$ , compared to hematite,  $R = 8$ . The difference between the dusts also reflects how much more reactive the kaolinite dust is than hematite, likely generating longer polymer

chains. The D<sub>5</sub> reaction on hematite shows that much more ozone is needed to facilitate reaction and the polymer chains are probably correspondingly shorter.

We investigated the combined effects of RH and O<sub>3</sub> on the decay of D<sub>4</sub> and D<sub>5</sub> for one of the mineral dusts, hematite. We have previously reported that modest amounts of RH, approximately 20%, significantly inhibited uptake of cVMS by hematite.<sup>22</sup> Similarly, ozone decomposition is greatly reduced as the RH is increased for the same hematite dust sample. In the mixture experiments, summarized in Figures 5 and 6, we also observe a reduction in the overall reaction extent as the RH is increased. The reaction extent can be expressed in terms of the fraction of the initial gas phase concentration that has reacted by the end of the experiment, after 400 min. The resultant fractions of cVMS and O<sub>3</sub> reacted at each RH are plotted in Figure 7. As can be seen in the figure, the overall uptake of both siloxane and ozone is reduced on the experimental time scale as the RH is increased. The reduction in the



**TABLE 2: Areal Rates for cVMS and O<sub>3</sub> Loss under Dry Conditions of Varying RH for Hematite Dust<sup>a</sup>**

RH		areal rate ( $\times 10^{10} \text{ cm}^{-2} \text{ s}^{-1}$ )		R
		cVMS	O <sub>3</sub>	
≤1%	D <sub>4</sub>	10 ± 2	1.2 ± 0.4	8 ± 5
	D <sub>5</sub>	2.4 ± 0.5	3.0 ± 0.7	0.8 ± 0.3
20%	D <sub>4</sub>	3.9 ± 0.5	1.9 ± 0.3	2.1 ± 0.6
	D <sub>5</sub>	1.6 ± 0.3	2.0 ± 0.5	0.8 ± 0.3
40%	D <sub>4</sub>	1.8 ± 0.4	1.7 ± 0.3	1.0 ± 0.4
	D <sub>5</sub>	0.6 ± 0.3	2.0 ± 0.5	0.3 ± 0.2
60%	D <sub>4</sub>	9 ± 2	1.9 ± 0.5	5 ± 2
	D <sub>5</sub>	1.6 ± 0.3	2.2 ± 0.6	0.7 ± 0.3
average	D <sub>4</sub>	6 ± 4	1.7 ± 0.8	4 ± 3
	D <sub>5</sub>	1.5 ± 0.7	2.3 ± 1.2	0.7 ± 0.5

<sup>a</sup> The ratio, *R*, of the cVMS to O<sub>3</sub> loss rates and the averages for each measurement have also been calculated.

ozone reaction is similar for either siloxane, suggesting that the effect of RH may act relatively independently on the two reactants. The D<sub>5</sub> appears to be somewhat less sensitive to RH than D<sub>4</sub> over the range of RH values we have explored, but the D<sub>5</sub> is already extremely reactive with the hematite surface, as we have noted. The adsorbed water, which is taken up the mineral dust surface on a much faster time scale than uptake of either ozone or cVMS,<sup>39,40</sup> appears to block active surface sites. In Figure 7, we have plotted a fit to water isotherm data reported for hematite samples using an ATR-FTIR technique.<sup>22</sup> The characteristic exponential decay time of cVMS or O<sub>3</sub>, which reflects initial uptake onto the surface, is inversely related to the number of available surface sites, according to eq 10

$$\tau \propto \frac{1}{\gamma_{\text{app}}[\text{S}]} \quad (10)$$

where [S] is the concentration of active surface sites. If the uptake coefficient,  $\gamma_{\text{app}}$ , does not change, then as the amount of surface adsorbed water increases with RH,<sup>41</sup> fewer surface sites are available and the decay time is longer, as we observe in Figures 5 and 6.

However, unlike our previous experiments that lacked ozone in the gas mixture, the current data show a characteristic linear decay for both the O<sub>3</sub> and the cVMS at longer times, indicating continued reactivity of the hematite surface at all RH values studied. The areal rates at each RH value were determined as described above, and the results are summarized in Table 2, along with the ratio of the cVMS to O<sub>3</sub> decay rate for each dust at each RH. Despite the presence of adsorbed water, the cVMS uptake continues, facilitated by the coadsorption of O<sub>3</sub>, which also continues to be lost from the gas phase. It is possible that the siloxane and ozone are able to displace surface adsorbed water and react. However, as we noted in our O<sub>3</sub>-hematite study,<sup>22</sup> the RH effect does not saturate at a monolayer coverage, which occurs at approximately 10% RH.<sup>22,41</sup> Instead, it may be that the water is not uniformly adsorbed onto the hematite surface, leaving unexposed areas with sufficient reactive sites to enable reaction, even at 60% RH where the coverage is expected to be on the order of 3–4 water monolayers.

The areal rates for both reactants are plotted as a function of RH in Figure 7. The ozone decay rates appear to be relatively independent of the RH, with an average value of  $(2.0 \pm 0.5) \times 10^{10} \text{ cm}^{-2} \text{ s}^{-1}$ . The corresponding rates for D<sub>4</sub> and D<sub>5</sub> do not display a simple monotonic dependence on RH. Both siloxanes

appear to exhibit areal rates that decrease with RH, reaching a minimum at approximately 40% RH, and then increasing again at the highest RH value studied, 60%. It is not clear if this behavior signifies a change in the reaction mechanism as the surface water content increases. At all RH values, the D<sub>4</sub> rate is larger than that of D<sub>5</sub>. Thus, just as under dry conditions, the reaction of D<sub>4</sub> requires less ozone to propagate. We have averaged the measured rates over all RH values in Table 2, along with the calculated ratio of cVMS rate to O<sub>3</sub> rate. On average, the D<sub>4</sub> reaction requires six times less ozone as D<sub>5</sub>, perhaps signifying the formation of longer linear polymers on the surface.

## Conclusion

The effect of coadsorbed ozone on the reactivity of the cVMS, D<sub>4</sub> and D<sub>5</sub>, toward two mineral dust samples, hematite and kaolinite, as well as carbon black was studied in an atmospheric reaction chamber. The presence of ozone opens up a new loss pathway for the siloxanes that is characterized by a linear decay of the gas phase species, signifying that the surface reaction is rate limiting. The O<sub>3</sub> appears to regenerate active surface sites on the mineral dust via an adsorbed product species, perhaps a surface oxide. The process is catalytic on the time scale of our experiments and the reaction does not terminate so long as cVMS and ozone are present in the chamber. Ozone only served to slightly reduce the reaction extent on carbon black, and no catalytic decomposition was observed. Increasing the RH in mineral dust experiments resulted in a suppression of the uptake of both O<sub>3</sub> and cVMS, and the measured reaction extent decreased. However, the same linear decay was still evident and the mineral dust surfaces continued to be reactive, even at 60% RH. Partitioning to the surface of mineral dust aerosol has been suggested to be a significant sink for gas phase D<sub>4</sub> and D<sub>5</sub> in the environment. The current results suggest that atmospheric oxidants, such as O<sub>3</sub>, may modify the mineral dust surface such that uptake of cVMS by mineral dust may be an even more important pathway. In particular, at RH values characteristic of the ambient atmosphere, the reaction with the dust does not saturate when O<sub>3</sub> is present. The overall loss rate may slow with increased RH, but the continuing reactivity of the surface due to a catalytic process facilitated by ozone means that more gas-phase siloxane can be lost to the dust surface.

**Acknowledgment.** This study was done at the University of Iowa with financial support provided by the Centre Europeen des Silicones (CES).

## References and Notes

- (1) Varaprath, S.; Frye, C.; Hamelink, J. *Environ. Toxicol. Chem.* **1996**, *15* (8), 1263–1265.
- (2) Flaningam, O. L. *J. Chem. Eng. Data* **1986**, *31* (3), 266–272.
- (3) Hobson, J. F.; Atkinson, R.; Carter, W. P. L. Part H. Organosilicon Materials In *The Handbook Environmental Chemistry*; Chandra, G., Ed.; Springer-Verlag: Berlin, 1997; Vol. 3.
- (4) Wang, X. M.; Lee, S. C.; Sheng, G. Y.; Chan, L. Y.; Fu, J. M.; Li, X. D.; Min, Y. S.; Chan, C. Y. *Appl. Geochem.* **2001**, *16* (11–12), 1447–1454.
- (5) Hamelink, J.; Simon, P.; Silberhorn, E. *Environ. Sci. Technol.* **1996**, *30* (6), 1946–1952.
- (6) Sousa, J. V.; McNamara, P. C.; Putt, A. E.; Machado, M. W.; Surrenant, D. C.; Hamelink, J. L.; Kent, D. J.; Silberhorn, E. M.; Hobson, J. F. *Environ. Toxicol. Chem.* **1995**, *14* (10), 1639–1647.
- (7) Xu, S. H.; Chandra, G. *Environ. Sci. Technol.* **1999**, *33* (22), 4034–4039.
- (8) Xu, S. *Environ. Sci. Technol.* **1999**, *33* (4), 603–608.
- (9) Allen, R. B.; Kochs, P.; Chandra, G. Part H. Organosilicon Materials In *The Handbook Environmental Chemistry*; Chandra, G., Ed.; Springer-Verlag: Berlin and Heidelberg, 1997; Vol. 3.



- (10) Atkinson, R. *Environ. Sci. Technol.* **1991**, 863–866.
- (11) Sommerlade, R.; Parlar, H.; Wrobel, D.; Kochs, P. *Environ. Sci. Technol.* **1993**, 2435–2440.
- (12) Karl, T.; Crutzen, P.; Mandl, M.; Staudinger, M.; Guenther, A.; Jordan, A.; Fall, R.; Lindinger, W. *Atmos. Environ.* **2001**, 35 (31), 5287–5300.
- (13) Atkinson, R. *Atmos. Environ.* **2000**, 2063–2101.
- (14) Whelan, M.; Estrada, E.; van Egmond, R. *Chemosphere* **2004**, 1427–1437.
- (15) Abe, Y.; Butler, G. B.; Hogenesch, T. E. *J. Macromol. Sci., Chem.* **1981**, A16 (2), 461–471.
- (16) Xu, S. H.; Lehmann, R. G.; Miller, J. R.; Chandra, G. *Environ. Sci. Technol.* **1998**, 32 (9), 1199–1206.
- (17) Latimer, H.; Kamens, R.; Chandra, G. *Chemosphere* **1998**, 2401–2414.
- (18) Liu, S. C.; Trainer, M.; Carroll, M. A.; Hubler, G.; Montzka, D. D.; Norton, R. B.; Ridley, B. A.; Walega, J. G.; Atlas, E. L.; Heikes, B. G.; Huebert, B. J.; Warren, W. *J. Geophys. Res., [Atmos.]* **1992**, 97 (D10), 10463–10471.
- (19) Chatfield, R. B. *Geophys. Res. Lett.* **1994**, 21 (24), 2705–2708.
- (20) Fan, S. M.; Jacob, D. J.; Mauzerall, D. L.; Bradshaw, J. D.; Sandholm, S. T.; Blake, D. R.; Singh, H. B.; Talbot, R. W.; Gregory, G. L.; Sachse, G. W. *J. Geophys. Res., [Atmos.]* **1994**, 99 (D8), 16867–16877.
- (21) Navea, J. G.; Xu, S.; Stanier, C. O.; Young, M. A.; Grassian, V. H. *Atm. Environ.* **2009**, doi:10.1016/j.atmosenv.2009.05.012.
- (22) Mogili, P. K.; Kleiber, P. D.; Young, M. A.; Grassian, V. H. *J. Phys. Chem. A* **2006**, 110 (51), 13799–13807.
- (23) Roscoe, J.; Abbatt, J. *J. Phys. Chem. A* **2005**, 109 (40), 9028–9034.
- (24) Li, W.; Oyama, S. *J. Am. Chem. Soc.* **1998**, 120 (35), 9047–9052.
- (25) Li, W.; Gibbs, G.; Oyama, S. *J. Am. Chem. Soc.* **1998**, 120 (35), 9041–9046.
- (26) Xi, Y.; Reed, C.; Lee, Y.; Oyama, S. *J. Phys. Chem. B* **2005**, 109 (37), 17587–17596.
- (27) Reed, C.; Lee, Y.; Oyama, S. *J. Phys. Chem. B* **2006**, 110 (9), 4207–4216.
- (28) Kwamena, N.; Thornton, J.; Abbatt, J. *J. Phys. Chem. A* **2004**, 108 (52), 11626–11634.
- (29) Kwamena, N.; Earp, M.; Young, C.; Abbatt, J. *J. Phys. Chem. A* **2006**, 110 (10), 3638–3646.
- (30) Mmerekki, B.; Donaldson, D.; Gilman, J.; Eliason, T.; Vaida, V. *Atmos. Environ.* **2004**, 38 (36), 6091–6103.
- (31) Mitchell, M.; Sheinker, V.; Cox, W. *J. Phys. Chem. C* **2007**, 111 (26), 9417–9426.
- (32) Prince, A.; Wade, J.; Grassian, V.; Kleiber, P.; Young, M. *Atmos. Environ.* **2002**, 36 (36–37), 5729–5740.
- (33) Orphal, J. *J. Photochem. Photobiol., A* **2003**, 157 (2–3), 185–209.
- (34) Curtis, D.; Meland, B.; Aycibin, M.; Arnold, N.; Grassian, V.; Young, M.; Kleiber, P. *J. Geophys. Res., [Atmos.]* **2008**, 113 (D8), doi:10.1029/2007JD009387.
- (35) Preszler-Prince, A. M. *Investigations into the heterogeneous atmospheric interactions of isolated metal oxide, carbonate and soot aerosols*. University of Iowa: Iowa City, IA, 2003.
- (36) Hanst, P. L.; Stephens, E. R.; Scott, W. E.; Doerr, R. C. *Anal. Chem.* **1961**, 33, 1113–15.
- (37) McAfee, J. M.; Stephens, E. R.; Fitz, D. R.; Pitts, J. N. *J. Quant. Spectrosc. Radiat. Transfer* **1976**, 16 (10), 829–837.
- (38) Bi, C.; Xiaoli, Z.; Lingmin, Y.; Fengqiu, C. *Chin. J. Chem. Eng.* **2007**, 15 (5), 661–665.
- (39) Seisel, S.; Lian, Y.; Keil, T.; Trukhin, M. E.; Zellner, R. *Phys. Chem. Chem. Phys.* **2004**, 6 (8), 1926–1932.
- (40) Seisel, S.; Pashkova, A.; Lian, Y.; Zellner, R. *Faraday Discuss.* **2005**, 130, 437–451.
- (41) Schuttlefield, J. D.; Cox, D.; Grassian, V. H., *J. Geophys. Res., [Atmos.]* **2007**, 112 (D21303), doi:10.1029/2007JD008973.

JP902192B